Fermi National Accelerator Laboratory

FERMILAB-Conf-93/360-E
CDF

Measurement of $\bar{p}p$ Elastic and Total Cross Section at $\sqrt{s}$ = 546 and 1800 Gev at CDF

Giorgio Chiarelli
For the CDF Collaboration

Laboratori Nazionali di Frascati, Frascati, Italy

Fermi National Accelerator Laboratory
P.O. Box 500, Batavia, Illinois 60510

November 1993

To be published in the Proceedings of the *9th Topical Workshop on Proton-Antiproton Collider Physics*, Tsukuba, Japan, October 18-22, 1993

Disclaimer

FERMILAB-CONF-93/360-E
CDF/PUB/PUBLIC/2329

Measurement of $\bar{p}p$ Elastic and Total Cross Section at $\sqrt{s}$=546 and 1800 GeV at CDF [1]

Giorgio Chiarelli
Laboratori Nazionali di Frascati
Via E.Fermi 40, 00044 Frascati-Italy
for the CDF Collaboration

Abstract

CDF measured the total, elastic and diffractive cross sections using the *luminosity independent* method. In this contribution we present the results for the total and elastic cross sections. CDF measured $(1+\rho^2)\cdot\sigma_{tot}$=62.64±0.95 (81.83±2.29) mb at $\sqrt{s}$=546 (1800) GeV. The elastic cross sections are 12.87±0.3 and 19.70±0.85 mb at the two energies. The elastic scattering data are well described by an exponential e^{bt}, with a slope b of 15.28±.58 (16.98±.25) GeV^{-2}

1 Experimental Method and Apparatus

The optical theorem relates the total cross section (σ_{tot}) to the value of the differential elastic cross section at $t = 0$. This allows a *luminosity independent* measurement of σ_{tot} via the simultaneous measurement of the total rate [2] and of the differential elastic rate dR_{el}/dt as a function of the four-momentum transfer squared (t). $(1+\rho^2)\cdot\sigma_{tot}$ is derived as:

$$(1) \quad (1+\rho^2)\cdot\sigma_{tot} = 16\pi(\hbar c)^2 \cdot \frac{dR_{el}/dt|_{t=0}}{R_{el}+R_{in}}$$

where ρ is the ratio of the real to the imaginary part of the forward elastic amplitude.

CDF data were collected during short dedicated runs in '88-'89. In order to perform the measurement we used part of the CDF detector, whose coverage was extended to smaller angle for both the inelastic and elastic measurement.

The elastic scattering was measured with a double arm magnetic spectrometer [3] which made use of the Tevatron magnetic lattice. The spectrometer consisted of five detectors along the Tevatron beam-line (z-axis). Each detector was composed of two *roman pots* symmetrically placed around the beam line. After beam injection, when stable operating conditions were reached, *roman pots* were moved towards the beam as close to as possible. Each pot comprised two scintillation counters for triggering, a drift wire chamber with x-y readout and a silicon detector (with double-sided readout in the plane transverse to the beam) (fig. 1). Elastically scattered $\bar{p}(p)$'s going through the west (east) side, were detected by S1,S2,S3 (S6,S7) of one of the two arms.

[1] To be published in the *Proceedings of the Topical Workshop on Proton-Antiproton Collider Physics* October 18-22, 1993. Tsukuba-Japan

[2] The total rate R_{tot} is defined as the sum of the elastic (R_{el}) and inelastic (R_{in}) rates. It is customary to divide the inelastic rate into non diffractive ($R_{non-diff}$) and diffractive (R_{diff}) contributions.

[3] Through this paper we will refer to the two independent arms as arm-0 and arm-1. Arm-0 detected elastic events due to $\bar{p}(p)$'s scattered outside(inside) of the beam orbit. Arm-1 detected symmetrically scattered elastic $\bar{p}$'s and p's.

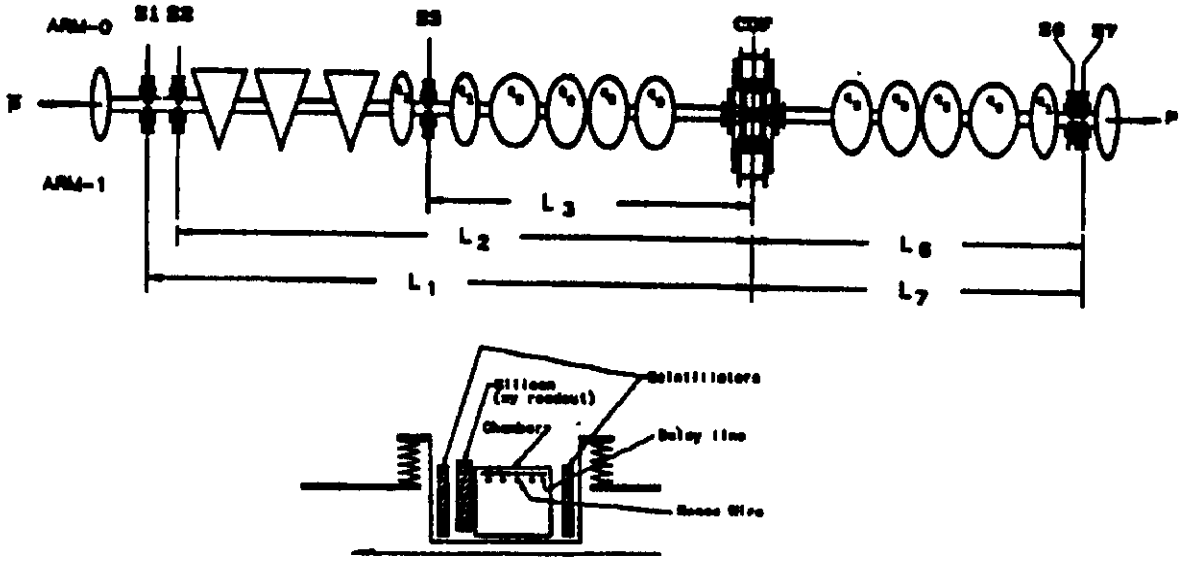

Figure 1: Top view of the elastic scattering set up. A sketch of *roman pot* is also shown

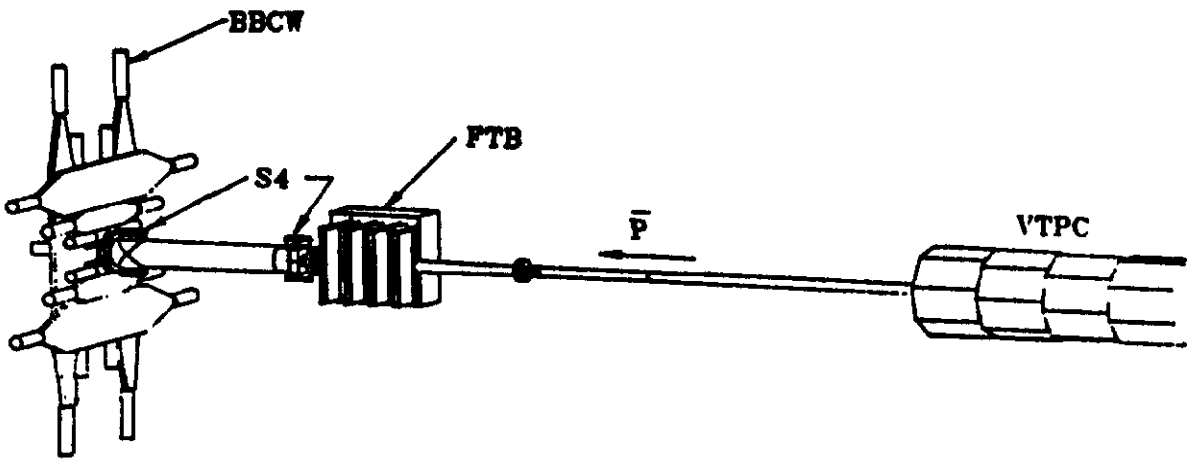

Figure 2: Layout of the inelastic detector. The west side (outgoing $\bar{p}$) only is shown.

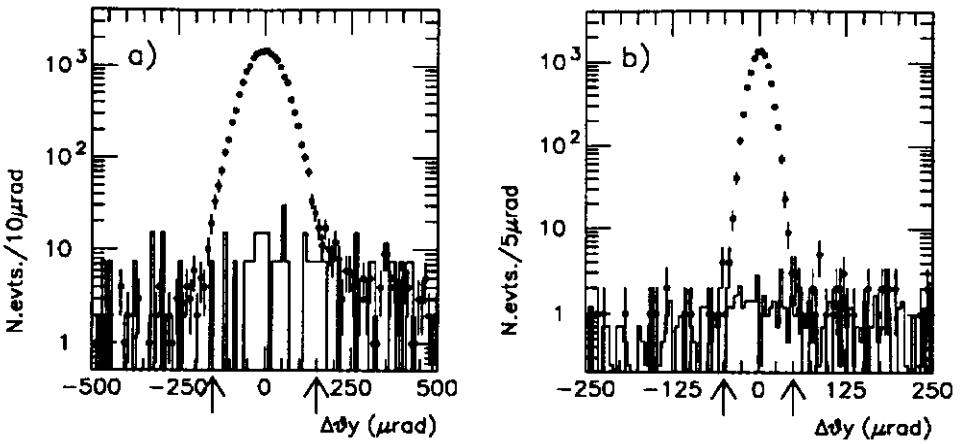

Figure 3: Collinearity distributions at a) $\sqrt{s}$=546 GeV and b) 1800 GeV. Solid lines indicate the background to be subtracted from data (•). Arrows indicate collinearity cuts.

The standard parts of CDF used for the inelastic measurement were the BBC counters (for triggering at $3.2 \leq |\eta| \leq 5.5$) and the VTPC (a set of 8 vertex time projection chambers covering $|\eta| \leq 3.5$). The angular coverage was extended to η=6.7 by scintillation counters placed inside *roman pots* S4 and S5, located at $\simeq 4m$ from the interaction point. S4 and S5 also contained drift chambers similar to the ones used in the elastic detector. Tracking capability was extended down to η of 6.7 by the drift chambers of S4 and S5 and by the two drift chambers telescopes FTF and FTB (see fig.2). The CDF detector has been described in [1], the elastic detector in [2,3] and the inelastic detector in [4].

The elastic event triggers were provided by the ten-fold coincidence of the scintillation counters sitting in each spectrometer arm. Inelastic events were collected with two different triggers: the *east* · *west* coincidence (BBCW+S4)*(BBCE+S5) used for the inelastic (non-diffractive) events and the $\bar{p}$ · *east* coincidence (S1*S2)*(BBCE+S5) which collected mostly single diffraction events.

2 Elastic scattering analysis

A detailed description of this analysis can be found in ref. [3]. Here an analysis summary is presented, before discussing the final results. First we rejected events due to satellite bunches and high multiplicity events due to nuclear interactions in the beam pipe and to beam losses. Then $\bar{p}$ and p tracks were reconstructed by using space points in each spectrometer detector. In events with more than one track, the ambiguity was solved by choosing the track pair with the best proton-antiproton collinearity. Events due to unambiguously identified beam-halo tracks were also removed. The final sample of events was obtained with a 3.5σ cut on the $\bar{p}$ impact-parameter distribution at the nominal interaction point and with a 4σ cut on the $\bar{p}p$ collinearity distribution. Fig. 3 shows the $\bar{p}p$ collinearity in the vertical coordinate for both energies. The residual background ($\leq$ .5%) was estimated from the tails of the collinearity distribution and statistically subtracted. Data were corrected for losses due to the analysis

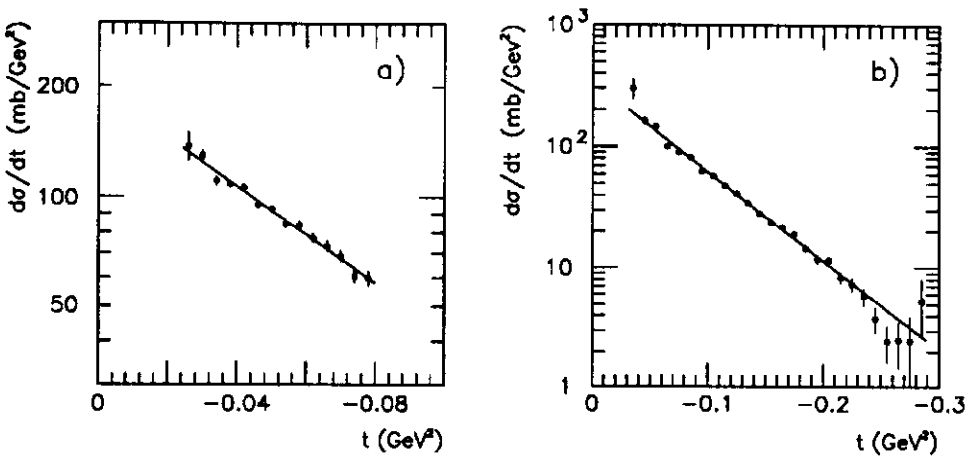

Figure 4: Differential cross section of proton-antiproton elastic scattering at (a) $\sqrt{s}$=546 GeV and at (b) $\sqrt{s}$=1800 GeV. Lines represent the fit results described in the text.

cuts and to nuclear interactions in the detectors. The raw t distribution was corrected for the geometrical acceptance and it was fit with the exponential form $A \cdot e^{bt}$. At 546 and 1800 GeV, data were corrected for the (small) Coulomb scattering contribution. At 546 GeV we also applied a correction for the smearing due to the t-resolution. The fit results for the slope are b=15.28±0.58(16.98±0.24) GeV^{-2} at 546 (1800) GeV. Fits are shown in Fig. 4. At 546 GeV, we improved the determination of the optical point by using also the more

Table 1: Systematical errors on b and A

	$\sqrt{s}$=546			$\sqrt{s}$=1800		
	A	b	N_{el}	A	b	N_{el}
Vertex cut	0.2		0.2	0.2		0.2
TOF losses	0.2		0.2	0.2		0.2
Background	0.2		0.2	0.2		0.2
Magnetic lattice	0.2	0.1	0.2	0.1	0.2	0.3
t_{min}	0.07		0.07	0.17		0.17
x-scale	0.1	0.1		0.1	0.1	
Tilt-angle	0.07	0.05	0.05	0.2	0.07	0.15
Nuclear interactions	0.2		0.2	0.2		0.2
Beam momentum	0.24	0.24		0.24	0.24	
b at $-t$ >0.25 GeV^2						0.2
Total	0.52	0.26	0.45	0.48	0.32	0.54

accurate b-values from the UA4 and UA4/2 experiments fitting our data with the additional constraint b=15.35±0.20 GeV^{-2}. The final statistical error on the optical point is 1.2 (3) % at $\sqrt{s}$=546 (1800) GeV. Using data and simulation we carefully studied the various sources of systematical errors (uncertainties in the event selection, background subtraction, nuclear

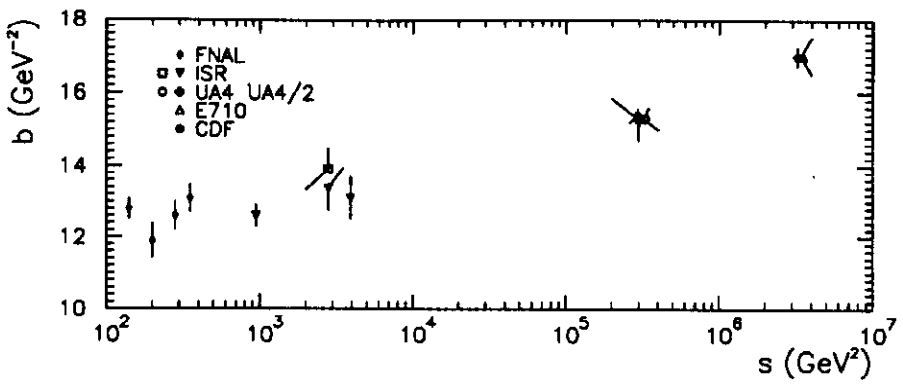

Figure 5: Elastic scattering slope as a function of s. Our results are shown together with other experiments in the same t-range.

interactions, t scale and offset, beam momentum spread) on b and A (Table 1). They yield a small contribution ($\simeq$ .3 % on the slope and $\simeq$ .5 % on the optical point at both energies) to the final results. In Fig.5 we compare our results for b to other $\bar{p}p$ experiments in a similar t-range. We fitted our results for the slope at 546 and 1800 GeV together with ISR results with the form $b = b_0 + 2 \cdot \alpha \cdot \log(s/s_0)$. The fit yields $\alpha = .26 \pm .02$ GeV^{-2}.

3 Analysis of the inelastic non-diffractive events

In this section we describe the main features of this analysis, a more extensive discussion can be found in ref.[4]. Events were collected by the *east* · *west* trigger which detected $\simeq$ 98 % of the inelastic (non diffractive) events and a small fraction of the high mass tail of single diffraction events due to the reaction $\bar{p}p \to \bar{p} + X$ and $\bar{p}p \to p + X$. Most of the background produced by beam halo or beam-gas interactions was removed using a time-of-flight cut and by using the VTPC capability to identify tracks due to showers originating upstream of the interaction region. In the events passing this selection all tracks with $|\eta| \leq 6.7$ were reconstructed. Tracks and timing information were used in order to reconstruct the event vertex. We studied the z event-vertices distribution for data and for Montecarlo simulated events in order to estimate the background (fig. 6). At 546 GeV there is no indication of residual background contamination. At 1800 GeV, where there is indication of residual background, we fitted the z-distribution of vertices reconstructed by the VTPC with a gaussian of fixed width, determined by the simulation, and a flat background. For event whose vertices were reconstructed in the forward telescope, the z-distribution was fit with a gaussian whose width was taken from simulation. For this set of events the beam-gas background shape for this events was determined using a set of tagged background events. After background subtraction, events were corrected for losses due to the partial angular coverage and to the requirement of a reconstructed vertex for validating the event.

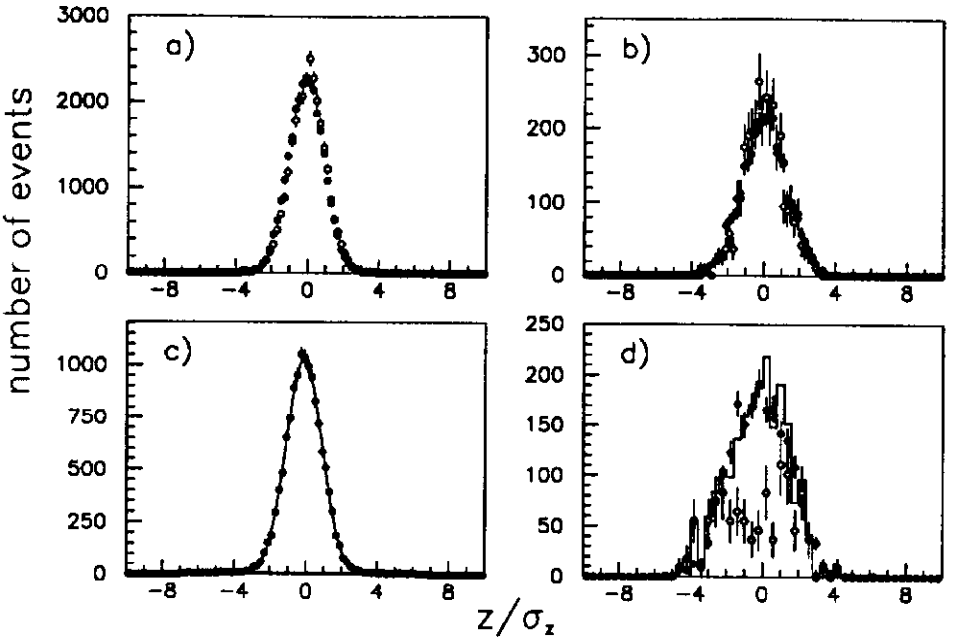

Figure 6: Vertex z-distributions in units of the spread σ_z.
Solid points (•) are data. a),c): VTPC.b),d):forward telescopes. a),b) $\sqrt{s}$=546 GeV: empty circles (o) are simulated inelastic events (normalized to the number of measured events). c),d) $\sqrt{s}$=1800 GeV: the solid line is the fit result. In d) the empty circles (o) indicate the estimate fraction of background.

4 Analysis of inelastic diffractive events

This analysis is subject of another contribution to this Workshop [5]. The only result needed for calculating the total cross section (i.e. the number of diffractive events) is listed in Table 2 along with the number of elastic and inelastic (non diffractive) events at the two energies and with the values of the extrapolation of the elastic rate to t=0.

Table 2: Contributions of the various triggers to the corrected total number of events.

		$\sqrt{s}$=546	$\sqrt{s}$=1800
Inelastic (W•E)	1	847796±8302	208890±2558
Inel. ($\bar{p}$•E): single diffr.	2	150151±7364	32092±1503
Total inelastic (1+2)		997947±11097	240982±2967
Elastic		265535±2411	78691±1463
$dN_{el}/dt\|_{t=0}$ (events/GeV^2)		4043598±52915	1336532±40943

5 Total and elastic cross sections

Using equation (1) and the numbers of events listed in Table 2, we obtain $(1+\rho^2)\cdot\sigma_T =$ 62.64 $\pm$ 0.95 and 81.83$\pm$2.29 mb at $\sqrt{s}$=546 and 1800 GeV. Assuming ρ=0.15, our results for the total cross section are 61.26 $\pm$0.93 at 546 and 80.03$\pm$2.24 mb at 1800 GeV. These results are in very good agreement with UA4 measurement at 546 GeV [6] and are larger than E710 measurement at 1800 GeV [7]. The elastic scattering cross sections are 12.87$\pm$0.30 (19.70$\pm$0.85) mb at $\sqrt{s}$=546 (1800) GeV. The ratio $r=\sigma_{el}/\sigma_{total}$ rises from 0.210$\pm$.002 at 546 GeV to 0.246 $\pm$0.004 at 1800 GeV, still far from the asymptotic regime of black-disc limit at which r=0.5. At the same time the central opacity of the nucleon, defined as $\mathrm{Im(f(s,B)}_{B=0}$ rises from 0.420$\pm$0.004 to 0.49$\pm$0.01 [4] almost reaching its unitarity bound of 0.5. Figure 7 shows our results for $\sigma_{el}, \sigma_{tot}$ and their ratio compared to other experiments.

References

[1] F.Abe et al. *The CDF Detector: An Overview,NIM* **A271**(1988)387;

[2] S.Bertolucci et al. *The Small Angle Spectrometer of CDF* NIM**A289** (1990),375.

[3] F.Abe et al., *Measurement of Small Angle Antiproton-Proton Elastic Scattering at $\sqrt{s}$=546 and 1800 GeV* Fermilab-Pub 93/232-E, Submitted to Phys. Rev.D.

[4] F.Abe et al., *Measurement of Antiproton-Proton Total Cross Section at $\sqrt{s}$=546 and 1800 GeV* Fermilab-Pub 93/234-E, Submitted to Phys. Rev.D.

[5] S.Miscetti *Precision Measurement of Single Diffraction Dissociation at sqrts=546 and 1800 GeV*,This Workshop.

[6] M.Bozzo et al.,*Measurement of the Proton-Antiproton Total Cross Section at the CERN SPS Collider* Phys. Lett.**147B**(1984),392.

[7] N.A.Amos et al.,*A Luminosity Independent Measurement of the $\bar{p}p$ Total Cross Section at $\sqrt{s}$= 1.8TeV*, Phys.Lett.**B243**(1990),158.

[4] f(s,B) is the forward elastic amplitude in terms of s and B, where B is the impact parameter.

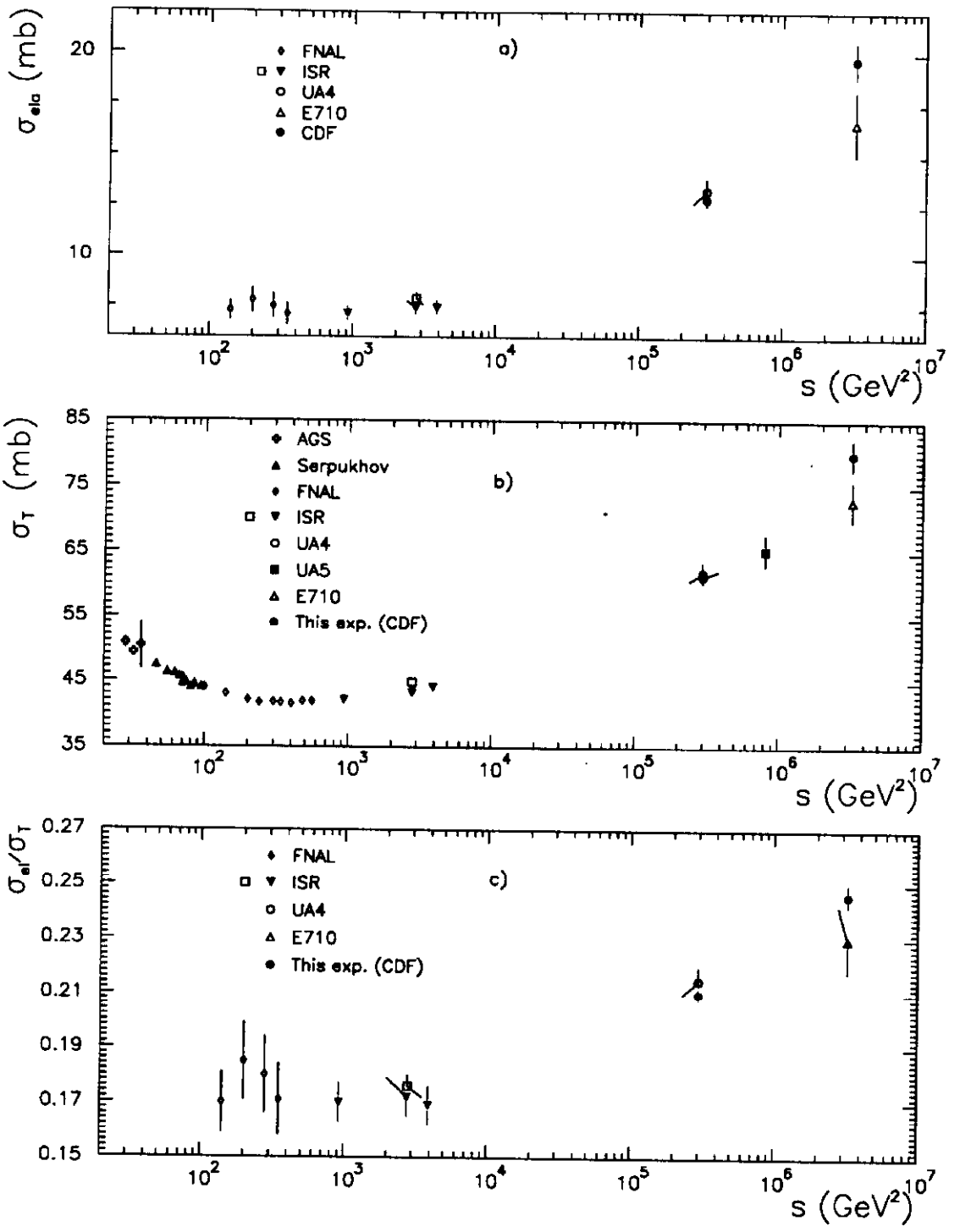

Figure 7: Our results for σ_{el} (a), σ_{tot} (b) and $\sigma_{ela}/\sigma_{tot}$ (c) compared to other $\bar{p}p$ experiment.